Remediation of Pb (II) ions from Kagara gold mining effluent using cotton hull adsorbent

M.D. Yahya [a], I. Yohanna [a], M. Auta [a], K.S. Obayomi [b],*

[a] *Department of Chemical Engineering, Federal University of Technology Minna, Niger State, Nigeria*
[b] *Department of Chemical Engineering, Landmark University Omu-Aran, Kwara State Nigeria*

ARTICLE INFO

ABSTRACT

Fixed-bed column adsorption experiment was conducted to remove lead ions from Kagara mining wastewater using unmodified Cotton Hull Adsorbent (CHA). Analysis of the wastewater effluent revealed that it contains as high as 85 mg/L lead ions. The Fourier Transform Infra-red, Brauneur-Emmet-Teller and Scanning Electron Microscopy characterization of the CHA revealed the presence of O-H, C–O, $C = O$, C–O-H and CH_2 functional groups, surface area of 139.8 m^2/g and porous micrograph of the adsorbent. The column flow experiment indicated that the maximum adsorption capacity of the carbon is 27.65 mg/g. Analysis of the experimental data using dynamic adsorption models revealed that Thomas model had insignificant difference between the average values of the experimental and the model's data. More so, it revealed high correlation coefficient of 0.77 to 0.96 signifying that Thomas model fitted adequately to the experimental data. This study has revealed that Kagara mining effluent which predominantly contains Pb ions can be sufficiently treated with unmodified cotton hull adsorbent before discharging it to the ecosystem.

Introduction

Heavy metals are metallic elements that have relatively high densities of ≥ 5 g/cm^3; many metals are needed by plants at micronutrient level while some of them (zinc, copper, selenium) are needed essentially by humans for adequate metabolism while some (cadmium, mercury, chromium, arsenic, thallium, and lead) in their low concentrations are poisonous or toxic to lives [1,2]. Lead metal ion like other heavy metals enters human bodies through potable water (lead piping), food and air (dust and rains) and then bioaccumulate. The duration and level of exposure of humans to this metal determines the intensity of effect caused. Saturnism or Lead poisoning may affect nervous system, kidneys, reproductive system, hemoglobin, joints, cognitive capability and children neuropsychological development [3,4].

Petrochemical and metallurgical processes, mining, electroplating, plastic, batteries, paper and pulp, and paint manufacturing wastewaters are major sources of lead pollution in the environment [5]. In many developing countries, lead exposure from mining activities is considered the primary source of the metal because the operation involves crushing, grinding and

flotation extraction processes of mineral ores which result into generation of huge volumes of wastewater and dust particles highly contaminated with lead element that further pollutes the surrounding environment [4].

The removal of heavy metals from contaminated soils can be achieved by various treatment methods such as chemical precipitation, ion exchange, and electrochemical removal. These processes which are generally known as conventional treatment methods have several disadvantages mainly due to high energy requirements, capital cost and low efficiency [6]. Remediation of lead ions poisoning have been undertaken by many researchers from polluted waters through batch [7] and column adsorption studies [8]. The quest for optimum removal of lead from wastewater engineered the study of various adsorbents viability with a view of getting a more efficient material.

Biodegradable, biocompatible, low toxic, renewable, deacetylated chitin product, chitosan has been widely applied for treatment of various effluents [9]. Chitosan-tripolyphosphate (CTPP) beads have been investigated for removal of Pb(II) and Cu(II) ions from aqueous. Thermodynamic analysis of the process revealed that the lead ion adsorption on the acidic (pH$_{zpc}$ 4.0) CTPP adsorbent was spontaneous, endothermic and had adsorption capacity of 57.33 mg/g. However, the chitosan flakes sample was purchased (Chito-Chem (M) Sdn. Bhd, Malaysia) and not synthesized [10].

Due to the sensitive nature of Pb (II) ions at very low concentrations, carbon nanotubes which is a chemically stable high surface area adsorbent that has reliable mechanical strength and which is very effective for determination of trace elements in solution or pre-concentration, have been applied [4,11]. Multi-walled CNTs (MCNTs) was produced, dispersed in grapheme oxide (GO) and further modified with di-ethylenetriamine (DETA),resulting in the GO–MCNTs–DETA used for the extraction of Pb (II) ions from wastewater. The adsorption of Pb (II) ions on GO–MCNTs–DETA adsorbent gave 6.6 mg/g adsorption capacity at a pH 4 [12].

Modified and unmodified cellulose have been applied for removal of heavy metal ions from wastewater. The unmodified cellulose adsorbent is characterized with variable physical stability and low heavy metal adsorption; halogenation, esterification, etherification and oxidation are some methods used to modify cellulose materials to enhance its adsorptive capability towards heavy metals [1]. A grafted copolymerization of acrylic acid onto wood pulp through γ-irradiation method was used for removal of Pb (II) and other metals from solutions and it gave maximum adsorption capacity of 6 mg/g for Pb ions [13].

Biosorption has recently attracted a considerable amount of attention as an alternative method used for the removal and recovery of toxic metals due to numerous advantages such as low sludge production, low investment, and operational cost and above all higher efficiency [14]. Thus, locally generated agricultural wastes such as cotton biomass have been tested in the production of activated carbon in many developing countries, though very few research works have been published in this regard [15].

This study focuses on the use of plant-based adsorbent produced from cotton seed hull for the adsorption of Pb (II) ions found in gold mining liquid effluent. Fixed-bed column flow adsorption experiment was conducted to investigate the effect of flow rate, bed height, and initial metal ion concentrations on breakthrough curves as well as adsorption kinetics of the Pb (II) ions in the mining waste solution onto the adsorbent.Some dynamic models were tested to further investigate the best fitted model to the empirical data generated.

Materials and method

The cotton hull (tough outer covering of cotton seed) was obtained from Funtua in Katsina, Nigeria. Sulphuric acid (98%), sodium carbonate (99%) were purchased from Gunsdong Chemicals-China, and Finar limited Gujarat-India, respectively. The chemicals were of analytical grade and used without further purification.

Preparation of cotton hull adsorbent

The cotton hull was obtained using a method reported by [16]. Typically, the cotton seed was sun dried to facilitate complete removal of fuzz from it and then delinted with H$_2$SO$_4$ at 100 mL/kg for 3 min and subsequently rinsed with deionized water. The delinted cotton seeds were neutralized with 2% Na$_2$CO$_3$ for 15 min, thoroughly washed with deionized water and then dried until 12% moisture content was attained. The dried seeds were de-hulled with the aid of mortar and pestle, sieved using 1–2 mm mesh size and handpicked to obtain hull free cotton seeds. The hull obtained was further dried at 105 °C for 12 h, pulverized, sieved using 500 μm mesh size and then packaged in air-tight sample pack for further use. The 500 μm pulverized sample was tagged cotton hull adsorbent CHA.

Characterization of cotton hull adsorbent

The morphology of the CHA was examined using scanning electron microscope DSM 9872 Gemni. A thin layer of the CHA was placed on the aluminum specimen holder with the aid of a double-sided tape coated with gold (AU) to about 3 nm thickness. The micrographs were recorded at various magnifications (500, 1000, 2000, 5000 and 10,000). To determine the functional groups present in the CHA, Fourier Transform Infra-Red (FTIR) spectroscopy Diamond ATR Agilent Cary 630. The CHA was mixed with potassium bromide (KBr) at 1:19, placed under hydraulic pressure equipment and pressed to prepare disc of the sample for analysis. The spectrum at 650–4000 cm^{-1} range CHA sample disc were determined and compared with the inbuilt library data for identification of the functional groups present. The surface area and porosity of the CHA were determined by Nitrogen adsorption procedure using Brauneur Emmett Teller BET (NOVA 4200E) analyzer. The

sample was first outgassed under vacuum at 200 °C for 3 h to remove contaminants and moisture content from it. The degassed sample was cooled before transferring it to a firmly fixed analyzing station of the equipment for further action using Nitrogen adsorption at 77 K.

Fixed-bed adsorption column study

A glass column measuring 30 cm and a diameter of 3 cm was used as the fixed-bed column. Glass wool layer was used at the bottom and top of the column support the CHA sample. To study the effect of CHA dosage different bed height of 2.7, 4 and 7 cm were used; while 5, 7.5 and 10 mL/min influent were varied to study the effect of lead effluent flow rate. More so, 50, 65 and 85 mg/L were used to study the effect of concentration on the breakthrough curves. An upward flow of the effluent into the column was adopted with the aid of peristaltic pump (Longer BQ50-IJ). Samples of the column experiment were collected at different time intervals and the residual concentration tested with the aid of Atomic Absorption Spectrophotometer until breakthrough point of the adsorption process was attained.

The effect of pH on the column adsorption was studied by using 0.1 M HCl solution to vary the solution pH from 2–10 in five different 250 mL capacity Erlenmeyer flasks at volume of 50 mL. The flasks were placed in a shaker set at 200 rpm. The residual concentration of the initial 85 mg/L lead effluent was determined after 2 h using Atomic Absorption Spectrophotometer.

Process evaluation of fixed-bed adsorption

The performance of a fixed-bed column was described through the concept of the breakthrough curve. The loading behavior of metal ions to be adsorbed from solution in a fixed-bed operation was expressed in terms of C_i/C_o as a function of time or volume of the effluent for a given bed height [17].

The total effluent volume treated by column adsorption was obtained using Eq. (1)

$$V_{eff} = Qt_{total} \tag{1}$$

Where, Q is the volumetric flow rate (ml/min), V_{eff} is the total effluent volume (ml), t_{total}, total flow time (min), C_i and C_o the feed effluent and influent concentration (mg/L) respectively.

The total mass of metal ions adsorbed in Column adsorptionq_{total} for a given feed concentrationand flow rate is equal to the area under the plot of the adsorbed metal concentration C_{ad} (mg/L) versus. t(min) as given by Eq. (2)

$$q_{total} = \frac{Q}{1000} \int_{t=0}^{t=t_{total}} C_{ad}dt \tag{2}$$

The total ions sent into a fixed bed column, m_{total} (mg):

$$m_{total} = \frac{C_oQt_{total}}{1000}. \tag{3}$$

Where C_o is the influent concentration (mg/l) and t_{total}, the total time of flow (min)

Percentage removal (% R) of Lead ions by column sorption was determined using Eq. (4)

$$\% R = \frac{q_{total}}{m_{total}}100\% \tag{4}$$

The amount of metal ions adsorbed at equilibrium, q_e (mg/g) was calculated by Eq. (5)

$$q_e = \frac{q_{total}}{m} \tag{5}$$

where m is the mass (g) of the adsorbent material

The adsorbent exhaustion rate, R_a (g/ml) was obtained using Eq. (6)

$$R_a = \frac{m}{V_{tb}} \tag{6}$$

Where V_{tb} (ml) is the volume of effluent treated at breakthrough

Results and discussions

Analysis of Kagara mining effluent

Elemental composition of the liquid effluent from Kagara mining site using Atomic Absorption Spectrophotometer revealed the presence of Zinc, Copper and Lead as shown in Table 1. Lead element was higher (85 mg/L) compared to other components. The disposal of such effluent poses significant threat to the environment and public health due to lead toxicity and its accumulation in the food chain [18]. Kagara mining effluent requires treatment using an inexpensive eco-friendly adsorbent before its discharge to the environment.

Table 1
Composition of Kagara gold mining effluent.

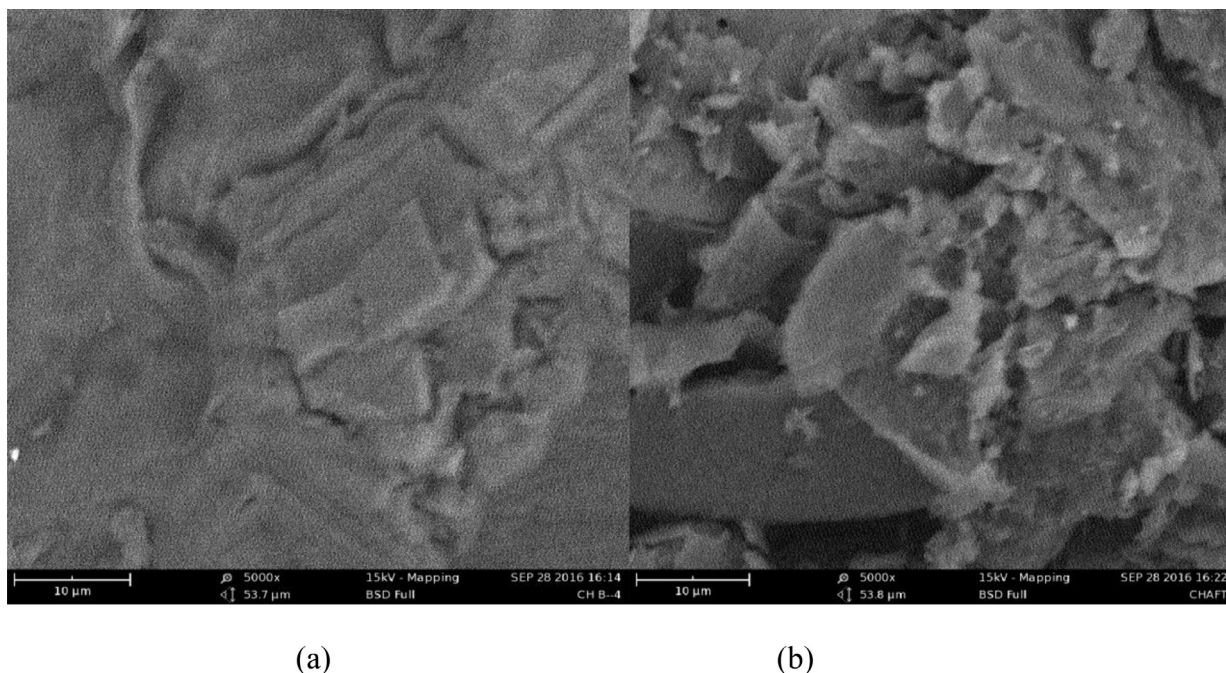| Parameter	Value
pH	7.4
Lead (mg/L)	85
Copper (mg/L)	2.5861
Zinc (mg/L)	0.4218

Fig. 1. Micrographs of cotton hull adsorbent before (a) and after (b) adsorption of Pb (II) ions.

Scanning electron microscopy (SEM) of cotton hull adsorbent (CHA)

The morphological structure of CHA before and after adsorption was determined using scanning electron microscopy analysis and the micrographs are presented in Fig. 1. At magnification of 5000 µm, the CHA surface texture and morphology were revealed clearly. Prior to the use of the CHA for adsorption operation, the pristine adsorbent surface was smooth and traces of microscopic pores and crevices. The CHA after adsorption became uneven and rough. The irregular appearance with formation of white layers could be attributed to presence of lead ions and foreign molecules deposition emanating from the effluent or weathering of the CHA by the flowing inlet solution during the column adsorption process [10].

Fourier transform infra-red analysis of CHA

The functional groups of CHA before and after adsorption were determined by FTIR spectroscopy analysis. Typically, peaks at wavelength of 3350, 1650 and 1200.2 cm^{-1}, are attributed to the presence of OH stretching, OH bending and C−O-C anti-symmetric stretching, respectively which are present in the CHA before and after usage for adsorption. The CHA before adsorption revealed five short bands within the range of 3947.3 and 3503.7 cm^{-1} which was associated with stretching vibrations of OH groups found in modified mesoporous carbon materials [19]. These short troughs within 3947.8 and 3503.7 cm^{-1} almost disappeared upon adsorption of Pb(II) ions on its surface except for the 3332.2 cm^{-1} peak. The presence of the OH$^-$ group enhanced the removal of Pb (II) through the surface reaction between the hydroxyl terminal and the Pb (II) [20]. This was further asserted by the presence of C−O functional groups which are polar in nature imparting high hydrophobicity on the adsorbent and generally exhibit high coordination with heavy metals, especially cations. Observation of the CHA surface after adsorption showed the shifting or vibration of some functional groups. There was a clear shift of wavenumber from 1699.7 to 1703.4 cm^{-1}, and 1580.4 to 1595.3 cm^{-1} due to high OH of water present in the spent adsorbent introduced by the effluent solution during the adsorption experiment. The finger print region vibrations in the range of 1025 to 670.2 cm^{-1} indicated interaction between Pb (II) ions with C−O, CH$_2$ and C−OH vibrations of the carbon materials (CHA).

Table 2
Vibrational modes assignment to components of fresh and Pb (II) loaded cotton hull.

Band assignment	Fresh adsorbent wave number (cm^{-1})	Pb(II) loaded adsorbent wave number (cm^{-1})
OH stretching	3947.3 to 3503.7	All disappeared only 3332.2 left
C≡C symmetric stretch	2366.9 and 2050.0	2366.9 Disappeared but 2050shifted to 2113.4
$C = C$ stretch	2016.5 and 1986.7	2016.5 disappeared but 1986.7shifted to 1997.9
OH bending and $C = O$ stretching	1699.7 and 1580.4	1699.7 shifted to 1703.4 and1580.4 cm^{-1} to 1595.3
H-C-H and O−C-H	1420.1	
C−O−C antisymmetric stretching	1200.2 cm^{-1} and 1155.5	1200.2 unchanged while1155.5 shifted to 1159.2
C-O stretch	1025	1028.7

Table 3
Physico-chemical characteristics of cotton hull adsorbent.

Parameter	Value
Apparent density (g/mL)	0.42
BET Surface area (m^2/g)	139.8
Micro-pore volume (cm^3/g)	0.0217
Pore radius (Å)	9.237

The C−O−C antisymmetric stretching of pyranose ring and glycosidic linkage revealed that these functional groups participated weakly in the adsorption experiment. This was due to the insignificant change observed in the spectra for the functional groups. A summary of the activities of the functional groups of the CHA before and after Pb (II) ion removal are summarized in Table 2.

The cotton hull adsorbent BET parameters analysis

The Brauneur-Emmet-Teller (BET) nitrogen adsorption result for the cotton hull sample is presented in Table 3. Specific surface area, pore volume and pore size of the cotton hull were determined in the BET analysis. Apart from the functional group playing vital role in the adsorption process, the extent of adsorption is also, related to the specific surface area of the adsorbent making its determination important in the study of adsorption process. The cotton hull material investigated exhibited a relatively high surface area of 139.8 m^2/g compared to some untreated agricultural adsorbents such as soy meal hull with 0.7623 m^2/g [21] and cotton seed shells with specific surface area 124.35 m^2/g [22]. The large specific surface area of the CHA showed (Table 3) that it contributed to high Pb (II) ions adsorption on the adsorbent. The high adsorption ability of the CHA was attributed to the larger micropore size of 9.237 Å of the adsorbent which allowed smaller lead atoms (3 Å diameter) to easily permeate its surface. However, the pore volume of CHA of 0.0217 cm^3/g presented in Table 3 could not retain large volume of the adsorbed heavy metal ions. Apparent density of the CHA was determined to evaluate the suitability of the adsorbent for water treatment processes. High apparent density value of the CHA materials of 0.42 g/mL suggests its feasibility for adsorption [23].

Analysis of effect of pH on lead ion adsorption

A pH 2 to 10 range was used to study its variation effect on the lead ion adsorption on CHA and the results presented in Fig. 2. The study of the removal of lead ion by CHA from the wastewater effluent revealed excellent uptake within the range of pH investigated. However, lower pH 2 did not promote the adsorption process which may be attributed repulsive activities between the increased hydrogen ion on the CHA and the lead ion present in the solution [24]. At pH>2, the greater number of the CHA functional groups promoted higher Pb (II) ion adsorption as can be seen in Fig. 2. At pH 5 and above for lead ion solutions, several hydroxyl low soluble species such as Pb(OH)$_2$ can be formed [25].

Column adsorption parameters studies

Effect of feed flow rate on breakthrough

The effect of inlet flow rate on lead ion adsorption was investigated by varying the feed flow rate (5, 7.5 and 10 mL/min) at constant bed height (4 cm) and inlet concentration (50 mg/L) as shown on the breakthrough curve in Fig. 4. The breakthrough point is that point in the adsorption zone of the column when the concentration of the pollutant, Pb (II) ions is observed in the outlet effluent. From this zone, adsorption is complete and the concentration of pollutant in the bed varies from 100% to approximately 0% of the initial concentrations. The breakpoint time is that time at which breakthrough occur. This adsorption zone moves downwards through the bed in relation to time until the breakthrough occurs. When the zone reaches the end of the bed, the pollutant in the effluent cannot be adsorbed any longer. This moment is called "saturated breakthrough" the plot obtained after this point gives the concentration history and is called breakthrough curve.
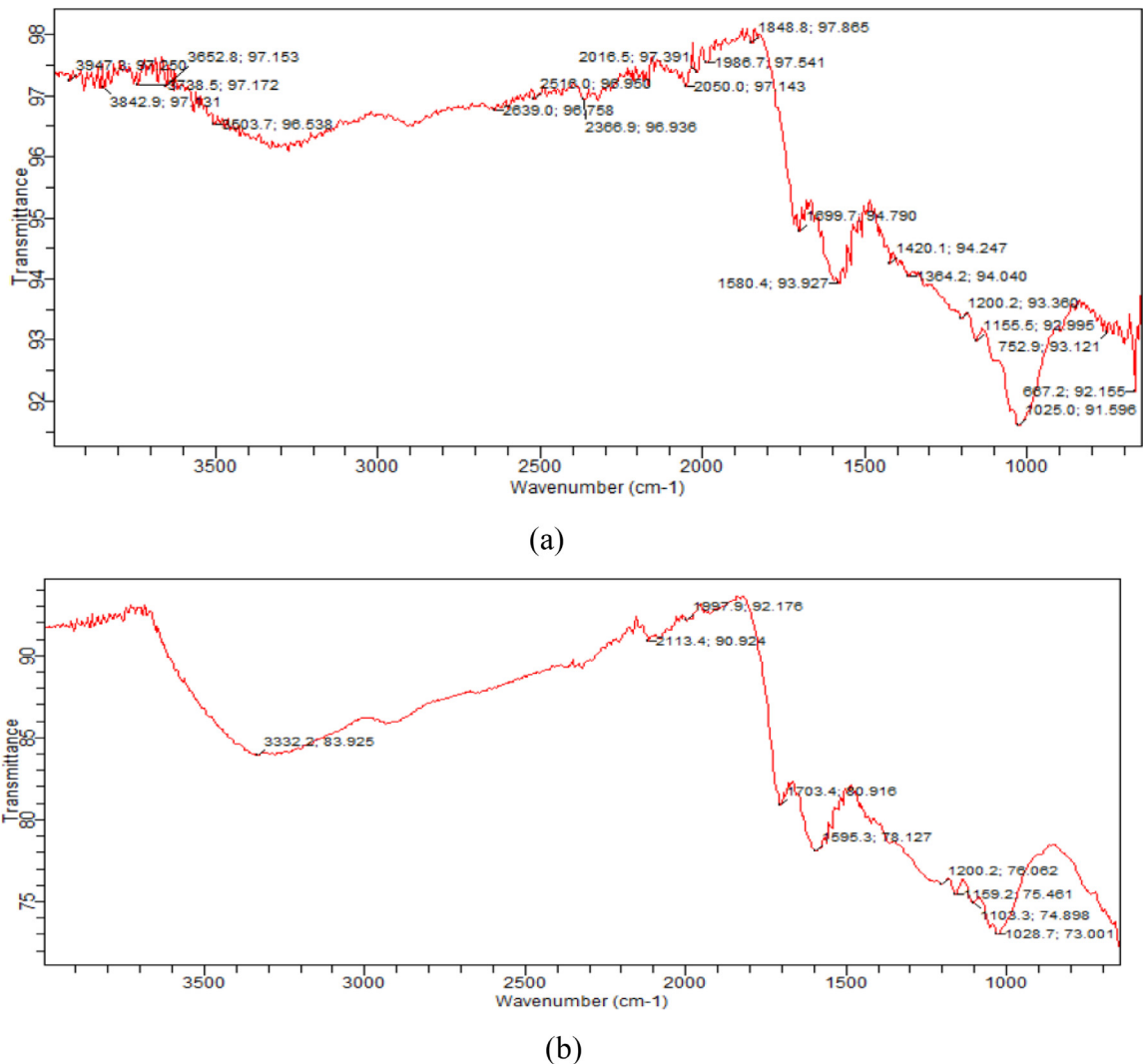
(a)

(b)

Fig. 2. The FTIR spectra of cotton hull adsorbent before (a) and after (b) Pb (II) ions adsorption.

Table 4
Evaluation of adsorption parameters using experimental data.

Q (ml/min)	Conc.(mg/L)	Bed height (cm)	q_e, exp(mg/g)	t_{total}(min)	V_b(ml)	t_{break}(min)	q_{total}(mg)	% removal	R_a (mg/ml)
5	50	4	27.65	3120	3605	721	780	50.68	3.967
7.5	50	4	25.58	2160	3600	480	810	45.16	3.972
10	50	4	19.56	1920	2400	240	960	29.14	5.958
5	65	4	24.01	2400	2400	480	780	44.02	5.958
5	85	4	20.05	1920	905	181	816	35.14	15.8
5	50	2.7	20.95	2160	310	62	540	41.12	34.19
5	50	7	23.81	3600	6060	1212	900	69.83	4.356

q_e experimental average = 23.09 mg/g and q_e theoretical average = 21.60 mg/g.

The breakthrough points time obtained were 721, 480 and 240 min for corresponding flow rates of 5, 7.5 and 10 mL/min; and saturated breakthrough time decreasing from 3120, 2160 and 1920 min, respectively. Increase in the flow rate from 5 to 10 mL/min led to decrease in percentage removal of Pb ions from 50.68 to 29.14%. Insufficient residence time of the effluent in the fixed bed operation due to high flow rate hog-tie the adsorption activities in the column. The breakthrough point and column saturation capacity times both decreased with increased in flow rate as presented in Table 4. These observations were in agreement with previous work reported on fixed-bed adsorption studies [26]. Graphical display of the effect of influent flow rate variation on the adsorption activities are presented in Fig. 3. Steeper profiles connoted lower percentage removal, breakthrough time, column saturation time and residence time. Potentials of Pb ions (solute) leaving the fixed bed
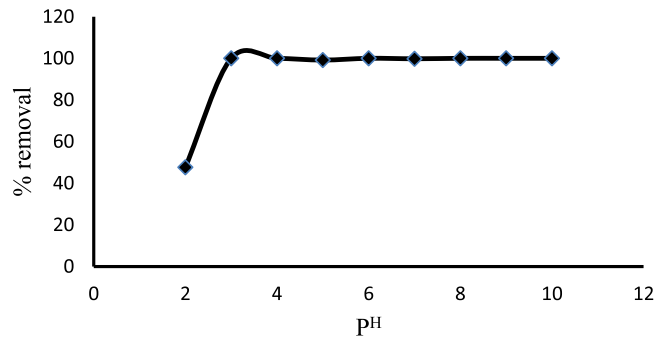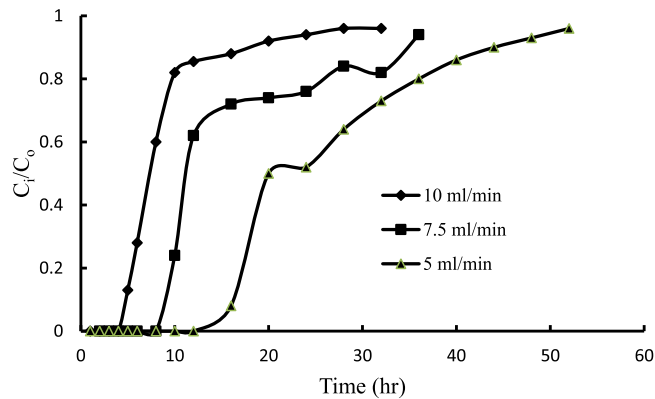
Fig. 3. Effect of pH on Lead ions adsorption.

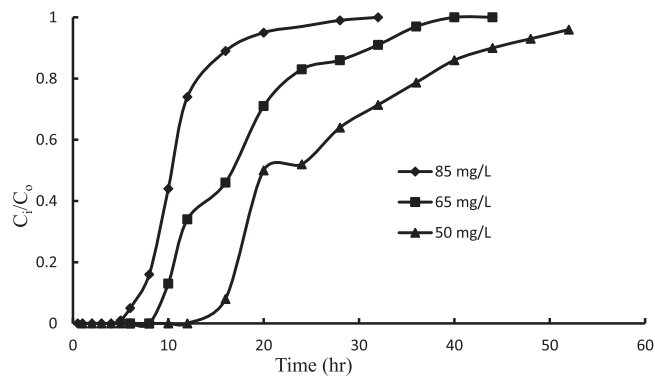**Fig. 4.** Effect of influent flow rate on Lead ions adsorption.

Fig. 5. Effect of initial influent concentration on Lead ions adsorptions.

column (outlet) was high at insufficient residence time which yielded lower adsorption capacity. A higher and outrageous flow rate promotes convective agitation and decrease in the thickness of the liquid film of the adsorbent [27].

Effect of initial concentration on Pb ion adsorption on CHA

Initial influent concentration variation (50, 65 and 85 mg/L) effect on breakthrough curves was studied at fixed flow rate (5 mL/min), pH 5 and bed depth (4 cm). The resulting breakthrough curves and adsorption parameters are presented in Fig. 5 and Table 4, respectively. Lower influent concentration gave longer breakthrough point time and CHA column exhaustion time which gave higher adsorption capacity as compared with higher initial Pb (II) ion concentration (Table 4). High mass of solute per unit area impinges on the surface of the adsorbent whenever fresh influent appears over the bed and the primary adsorption zone mobilizes rapidly across the bed. However, these activities are more prominent at higher influent concentration resulting to faster breakthrough point and column saturation appearance. The higher percentage removal of the Pb ion at lower influent concentration despite a decrease in the diffusion coefficient or the mass transfer coefficient is
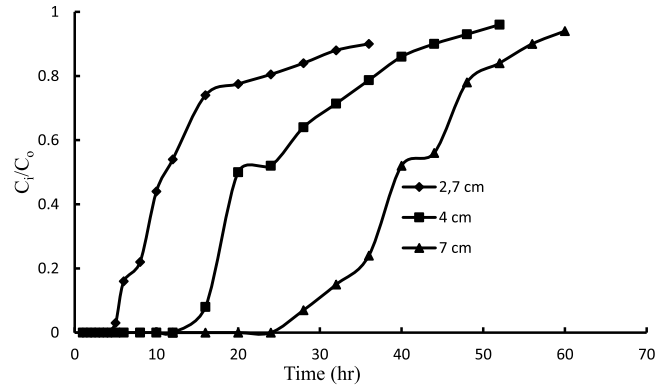
Fig. 6. Effect of bed height on Lead ions adsorption.

Table 5
Thomas model parameters at different conditions using regression analysis.

Q_f (ml/min)	Conc.(mg/L)	Bed height (cm)	t_{total}(min)	V_{eff} (ml)	K_{TH} (ml/mg.min)	q_{Th} (mg/g)	q_e, exp(mg/g)	R^2
5	50	4	3120	15,600	0.042	27.25	27.65	0.9021
7.5	50	4	2160	16,200	0.036	18.93	25.58	0.7883
10	50	4	1920	19,200	0.054	14.9	19.56	0.7741
5	65	4	2400	12,000	0.046	23.02	24.01	0.9551
5	85	4	1920	9600	0.068	22.92	20.05	0.9028
5	50	2.7	2160	10,800	0.07	19.7	20.95	0.7674
5	50	7	3600	18,000	0.068	24.46	23.81	0.9261

due to the presence of ample and optimum solute molecules present in the solution that were gradually and consecutively adsorbed by the commensurate yearning active sites present on the CHA [28].

Effect of bed height on CHA adsorption

Variation of bed height connotes variation of active sites of the adsorbent per unit mass. The bed height of the CHA adsorbent was varied (2.7, 4, & 7 cm) at fixed influent flow rate (5 mL/min) and concentration (50 mg/L) to study its effect on the Pb ion adsorption operation. The breakthrough profiles and the parameters are presented in Fig. 6 and Table 4. Longer bed heights (7 cm) increased the specific surface area of the CHA which provided more fixations of the cations with active binding sites for promotion of the adsorption activities. This resulted to higher adsorption capacity (27.65 mg/g) due to larger service area of CHA, higher volume of the treated Pb effluent, longer breakthrough point and column saturation time, and less steeper slopes of the breakthrough curve [8].

Dynamic column adsorption models analysis

The time for breakthrough appearance and the shape of the breakthrough curve are very important features for determining the operation and the dynamic response of an adsorption column.

Evaluation of Thomas model for Pb ion adsorption on CHA

The Thomas Model parameters for the removal of Pb ions on the surface of CHA adsorbent are presented on Table 5. It was observed that increase in the initial influent concentration was directly proportional to the increase in the Thomas model constant K_{th} (0.042 to 0.068 mL/mg.min) but inversely proportional to the decrease in uptake capacity q_{th} (27.25 to 22.92 mg/g). When fluid flow rate increases, there is always a tendency of high system turbulence which minimizes film diffusion effects and hence low solute ions uptake. Table 5 reveals that the difference between the average experimental uptake (23.09 mg/g) and the average value predicted from Thomas model (21.60 mg/g) can be considered insignificant and the correlation values were reasonably high ($0.7674 \leq R^2 \leq 0.9551$).

Application of Yoon-Nelson in investigating adsorption data

The Yoon-Nelson adsorption model parameters k_{YN} and τ for Pb ions removal by CHA are presented in Table 6. It was observed that at constant flow and bed length, values of model constant, k_{YN} were found to increase from 0.0021 to 0.0058 per minute with increase in initial concentration but the time required to retain the Pb ion breakthrough of 50% (min) denoted by "τ" values instead decreased [29]. The greater change in values of the Yoon-Nelson rate constant, k_{YN} when the inlet lead concentration is made higher may be related to the increase in the forces that control the mass transfer

Table 6
Adsorption data to investigate fitness of Yoon-Nelson.

Qf(ml/min)	Conc.(mg/L)	Bed height(cm)	K_{YN} (1/min)	τ(min)	R^2	τ_{exp} (min)
5	50	4	0.0021	1559.2857	0.9031	1442
7.5	50	4	0.0017	751.8823	0.7881	960
10	50	4	0.0027	417.6296	0.7661	480
5	65	4	0.003	1009.4667	0.9551	960
5	85	4	0.0058	768.5345	0.9028	362
5	50	2.7	0.0034	1098.0294	0.7865	124
5	50	7	0.0034	2572.2941	0.9244	2424

in the liquid phase. However, the 50% breakthrough time, τ significant decrease when the initial concentration increases was attributed to rapid saturation of the column due to presence of more solute molecules. Invariably, the values of τ increased (1098.03 to 2572.29 min) with increase in bed height (2.7 to 7 cm), whereas values of K_{YN} decreased as shown in Table 6. This is similar to report on adsorption by other researchers [30,31]. The predicted 50% breakthrough times, τ was reasonably in agreement with experimental data for all flow rates, bed heights and the initial lead concentration; the correlation coefficient, R^2 values ($0.7062 \leq R^2 \leq 0.9155$) predicted good fit for the model.

The applicability of Thomas and Yoon-Nelson dynamic models for adsorption of Pb ions on CHA showed that both models suitably described the process due to the high correlation coefficients values which were $0.70 \leq R^2 \leq 0.90$. However, critical analysis of the predicted and experimental data of two models revealed the Yoon-Nelson predicted breakthrough times, τ values were largely at variance. Whereas the predicted and experimental adsorption capacity were comparably close with insignificant variations recorded. This evaluation revealed that Thomas dynamic model best described the Pb ion adsorption on CHA which connotes that the process obeys second order kinetics with the film interface mass transfer as the reaction rate limiting step.

Conclusion

Cotton seed hull adsorbent (CHA) was produced and successfully tested as an alternative sorbent for the removal of Pb (II) metal ions from solution. The adsorbent has numerous functional groups, high apparent density and relatively high surface area (138.9 m^2/g) when compared with other untreated adsorbent materials. The column adsorption studies revealed that shape of the breakthrough curves was greatly influenced by the influent flow rate, bed depth and initial concentration. On the strength of evaluation of dynamic models using the data generated experimentally, Thomas model described the adsorption process better denoting that film interface mass transfer was the reaction rate limiting step for the second order kinetics activities exhibited by the system.

Declaration of Competing Interest

The Author's declared that there is no conflict of interest.

References

[1] D.W. O'Connell, C. Birkinshaw, T.F. O'Dwyer, Heavy metal adsorbents prepared from the modification of cellulose: a review, Bioresour. Technol. 99 (2008) 6709–6724.
[2] R.M. Ali, H.A. Hamad, M.M. Hussein, G.F. Malash, Potential of using green adsorbent of heavy metal removal fromaqueous solutions: adsorption kinetics, isotherm, thermodynamic, mechanism and economic analysis, Ecol. Eng. 91 (2016) 317–332.
[3] A. Witek-Krowiak, R.G. Szafran, S. Modelski, Biosorption of heavy metals from aqueous solution onto peanut shell as a low-cost biosorbent, Desalination 265 (2011) 126–134.
[4] A. Ihsanullah, Aamir Abbas, A.M. Al-Amer, T. Laoui, M.J. Al-Marri, M.S. Nasser, M. Khraisheh, M.A. Atieh, Heavy metal removal from aqueous solution by advanced carbon nanotubes: critical review of adsorption applications, Sep. Purif. Technol. 157 (2016) 141–161.
[5] I. Oboh, E. Aluyor, T. Audu, Biosorption of heavy metal ions from aqueous solutions using a biomaterial, Leonardo J. Sci. 14 (2009) 58–65.
[6] M.A. Barakat, New trends in removing heavy metals from industrial waste water, Arab. J. Chem. 4 (2011) 363.
[7] Y.-.S. Ho, A.E. Ofomaja, Pseudo-second-order model for lead ion sorption from aqueous solutions onto palm kernel fiber, J. Hazard. Mater. B129 (2006) 137–142.
[8] V.C. Taty-Costodes, C. Porte, Y.S. Ho, Removal of lead (II) ions from synthetic and real effluents using immobilized *Pinus sylvestris*sawdust: adsorption on a fixed-bed column, J. Hazard. Mater. B123 (2005) 135–144.
[9] M. Auta, B.H. Hameed, Coalesced chitosan activated carbon composite for batch and fixed-bed adsorption of cationic and anionic dyes, Colloids Surf. B (2013) 199–206.
[10] S. Fatinathan, W.S Wan Ngah, Adsorption characterization of Pb(II) and Cu(II) ions onto chitosan-tripolyphosphate beads: kinetic, equilibrium and thermodynamic studies, J. Environ.Manag. 91 (2010) 958–969.
[11] T.C. Egbosiuba, A.S. Abdulkareem, A.S. Kovo, E.A. Afolabi, J.O. Tijani, M. Auta, W.D. Roos, Ultrasonic enhanced adsorption of methylene blue onto the optimized surface area of activated carbon: adsorption isotherm, kinetics and thermodynamics, Chem. Eng. Res. Des. 153 (2020) 315–336.
[12] X. Zhu, Y. Cui, X. Chang, H. Wang, Selectivesolid-phaseextractionandanalysisoftrace-level Cr(III), Fe(III), Pb(II),and Mn(II) ions in wastewater using diethylenetriamine-functionalized carbon nanotubes dispersed in graphene oxide colloids, Talanta 146 (2016) 358–363.
[13] S.E. Abdel-Aal, Y. Gad, A.M. Dessouki, The use of wood pulp and radiation modified starch in wastewater treatment, J. Appl. Polym. Sci. 99 (2006) 2460–2469.

[14] S. Amirnia, M.B. Ray, A. Margaritis, Copper ion removal by Acer saccharum leaves in a regenerable continuous-flow column, Chem. Eng. J. 287 (2016) 755–764.
[15] Z. Ding, X. Hu, A.R. Zimmerman, B. Gao, Sorption and cosorption of lead (II) and methylene blue on chemicallymodified biomass, Bioresour. Technol. 167 (2014) 569–573.
[16] N.K. Biradarpatil, M. Sangeeta, Effect of dosages of sulphuric acid and duration of delinting on seed quality in desi cotton, Karnataka J. Agric. Sc. 22 (4) (2008) 896.
[17] Z. Aksu, F. Gonen, Biosorption of phenol by immobilized activated sludge in a continuous packed bed: prediction of breakthrough curves, J. Process Biochem. 39 (2004) 601 2004.
[18] B. Paul, G. Clement, Y.K. Patlolla, D.J Sutton, Heavy metals toxicity and the environment, PubMed Central Journal 101 (2014) 133.
[19] H. Hamad, Z. Ezzeddine, F. Lakis, H. Rammal, M. Srour, A. Hijazi, An insight into the removal of Cu (II) and Pb (II) by aminopropylmodified mesoporous carbon CMK-3: adsorption capacity andMechanism, Mater. Chem. Phys. 178 (2016) 57–64.
[20] S.L. Iconaru, M.M. Heino, R. Guegan, M. Beuran, A. Costescu, D. Predoi, Adsorption of Pb (II) ions onto hydroxyapatite nanopowders in aqueous solutions, J. Mater. (2018).
[21] M. Arami, N.Y. Limaee, N.M. Mahmoodi, N.S. Tabrizi, Equilibrium and kinetics studies for the adsorption of direct and acid dyes from aqueous solution by soy meal hull, J. Hazard. Mater 135 (2006) 171–179.
[22] N. Thinakaran, P. Panneerselvam, P. Baskaralingam, D. Elango, S. Sivanesan, Equilibrium and kinetic studies on the removal of acid red 114 from aqueous solutions using activated carbons prepared from seed shells, J. Hazard. Mater. 158 (2008) 142–150.
[23] O.H. Ekpete, Preparation and characterization of activated carbon derived from fluted pumpkin stem waste (Telfairiaoccidentalis hook F), Res. J. Chem. Sci. 1 (2011) 10–17.
[24] M.M.S. Saif, K.N. Siva, M.N.N Prasad, Binding of cadmium to strychnospotatorum seed proteins in aqueous solution: adsorption kinetics and relevance to water purification, Colloids Surf. B 94 (2012) 75–78.
[25] P. Loderio, R. Herreo, M.E. Sastre de Vicentes, The use of protonated sargassum muticum as biosorbent for cadmium removal in a fixed-bed column, J. Hazard. Mater. 137 (2006) 247.
[26] M. Auta, B.H. Hameed, Acid modified local clay beads as effective low-cost adsorbent for dynamic adsorption of methylene blue, J. Ind. Eng. Chem. 19 (2013) 1153–1161.
[27] J.M.P.Q Delgado, A critical review of dispersion in packed beds, Springer-Verlag 42 (2006) 285.
[28] S.R. Shukla, V.G. Gaikar, R.S. Pai, Batch and column adsorption of Cu(II) on unmodified and oxidized coir, J. Environ. Sci. Tecnol. 44 (2009) 40.
[29] A.A. Ahmad, B.H. Hameed, Fixed-bed adsorption of reactive azo dye onto granular activated carbon prepared from waste, J. Hazard. Mater. 175 (2010) 298–303.
[30] R. Han, D. Ding, Y. Xu, W. Zou, Y. Wang, Y. Li, L. Zou, Use of rice husk for the adsorption of congo red from aqueous solution in column mode, Bioresour. Technol. 99 (2008) 2938–2946.
[31] R. Han, Y. Wang, X. Zhao, Y. Wang, F. Xie, J. Cheng, M Tang, Adsorption of methylene blue by phoenix tree leaf powder in a fixed-bed column: experiments and prediction of breakthrough curves, Desalination 245 (2009) 284–297.